July 2002

ELSEVIER

Materials Letters 55 (2002) 1–7

MATERIALS LETTERS

www.elsevier.com/locate/matlet

The influence of Yb concentration on laser crystal Yb:YAG

Hongwei Qiu*, Peizhi Yang, Jun Dong, Peizhen Deng, Jun Xu, Wei Chen

Shanghai Institute of Optics and Fine Mechanics, The Chinese Academy of Sciences, Shanghai 201800, People's Republic of China

Received 20 April 2001; accepted 10 August 2001

Abstract

The thermal properties, absorption spectra and Raman spectra of Yb:YAG crystal with different Yb^{3+} ion concentrations are reported. The results show that the ytterbium concentration influences the properties of Yb:YAG. At high doping level, the thermal conductivity decreases and the absorption peak centered at about 940 nm shifts to shorter wavelength. The Raman spectra reveal that the lattice vibrational modes of highly doped Yb:YAG is different from that of low-doped Yb:YAG crystal. The effect of Yb^{3+} concentration on the properties is regarded as the result of lattice deformation. The influence of Yb concentration on laser is also analyzed.

PACS: 42.55–f

Keywords: Yb:YAG; Laser; Thermal conductivity; Absorption spectra; X-ray diffraction; Raman spectra; Crystal lattice deformation

1. Introduction

Because laser diode (LD) pumped solid-state lasers can offer many desirable properties such as compact, high efficient laser performance, they become the main developing direction of solid-state lasers [1,2]. And the recent advances of diode lasers with wavelength between 900 and 1100 nm have stimulated interest in developing LD pumped Yb^{3+} doped lasers. Owing to its simple electronic structure based on two electronic manifolds, the ground $^2F_{7/2}$ state and an excited $^2F_{5/2}$ state, Yb^{3+} has advantageous spectroscopic properties especially suited for diode-pumping schemes [3–6]. First, ytterbium generally has long storage lifetime, which is approximately four times longer than that of its Nd-doped counterparts. Second, Yb^{3+} ion-doped materials exhibit broad absorption bands (FWHM). So there is no need to precisely control the temperature of diode. Third, the simple electronic structure in near-infrared spectra leads to a low quantum defect, excited state absorption, and nonradiative decay. These reduce the thermal load and thermal problems. The absence of additional 4f levels in Yb^{3+} also eliminates the effects of upconversion, concentration quenching, so highly doped Yb:YAG crystals can be grown without concentration quenching.

More attention has been paid to the Yb:YAG crystal because of the good thermal, physical, chemical properties and laser characteristics of YAG—especially high quality and highly doped Yb:YAG crystals can be grown using traditional Czochralski (CZ) method.

But until now, the data of thermal conductivity and absorption peak wavelength used to design the system of laser experiments are of pure YAG [4], or of low-doped Yb:YAG [7]. Some properties of Yb:YAG

* Corresponding author. Fax: +86-21-59928755.
E-mail address: qhongwei@163.net (H. Qiu).

0167-577X/02/$ - see front matter
PII: S0167-577X(01)00608-5

crystals have been changed with the increase of the Yb^{3+} concentration in Yb:YAG crystals, so we need to reconsider the properties of highly doped Yb:YAG crystals so that we can design LD pumped Yb:YAG lasers properly. The purpose of this paper is to investigate the influence of doping concentration on the thermal, spectra, and laser properties of Yb:YAG. First, in Section 2 the experimental procedures are described, and the results of our measurements are presented and discussed in Section 3. In Section 4, we analyze the influence of doping concentration on the laser performance of Yb:YAG. The conclusion is stated in the Section 5.

2. Experimental

2.1. Crystal growth

The ⟨111⟩-oriented Yb:YAG crystals were grown from Ir crucibles in an atmosphere of N_2 by the Czochralski technique. High-purity raw oxide materials are used. The pulling rate was 2–3 mm/h and rotation rate was about 20 rpm. Because there are color centers and residual stress in as-grown Yb:YAG crystals, the annealing process is necessary. The annealing process is as following: in pure oxygen, the crystals were fired at 1600 °C for 18 h, and cooled to room temperature at a rate of 10 °C/h. After annealing, the crystals are all colorless. The lattice parameters were measured by an RAX-10 X-ray diffractometer.

2.2. The measurement of thermal properties

The specific heat was measured by the method of differential scanning calorimetry (DSC). The instrument used was DSC-50 DSC, which had the cooling system of LTC-50. The resolution is 1% and the temperature increase rate is 10 °C/min. Thermal diffusivity was measured from 25 to 300 °C by pulsed laser technique with a Xe lamp pumped Nd:Glass laser. The samples are $\phi 10 \times (1-2)$ mm 5 and 30 at.% doped Yb:YAG crystals.

2.3. Spectral measurement

The absorption spectra were measured on the Lambda 9UV/VIR/NIR spectrophotometer at room temperature. The thickness of the samples was 4 mm. Room temperature Raman spectra were measured on LabRam-IB Raman spectrometer with a slit width of 100 μm, a 6-mW He–Ne laser at 632.8-nm wavelength was used as pumping source. The Raman spectra with a resolution of 1 cm^{-1} were measured in the range from 500 to 1200 cm^{-1}. The concentrations of the samples were 5 and 30 at.%. The laser pump source was vertical to the (111) and $(1\bar{1}0)$ face, respectively, and the signal was received from the same direction.

3. Results and discussion

3.1. Thermal properties

The specific heat (C_p) of 5 and 20 at.% doped Yb:YAG are shown in Fig. 1. It shows that C_p of Yb:YAG decreases with the increase of Yb^{3+} concentration in the range from room temperature to 200 °C. When the temperature exceeds 200 °C, C_p of highly doped Yb:YAG crystal is higher than that of low-doped Yb:YAG crystal, at the same time C_p of highly doped Yb:YAG crystal increases more quickly than that of low doped Yb:YAG crystal in the whole range of experimental temperature from room temperature to 300 °C. The results show that the variety of temperature has great influences on high-doped Yb:YAG crystals.

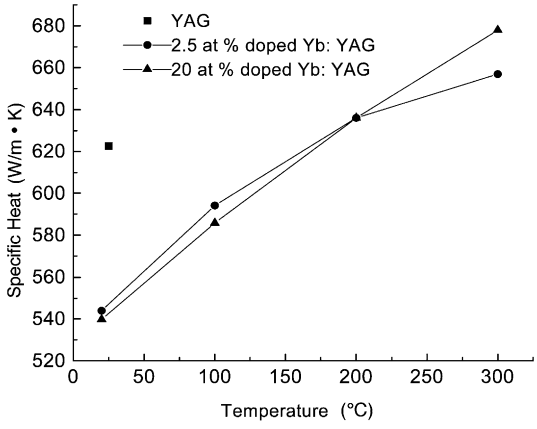

Fig. 1. Specific heat of Yb:YAG with Yb^{3+} concentration of 2.5 and 20 at.% (■— specific heat of YAG).

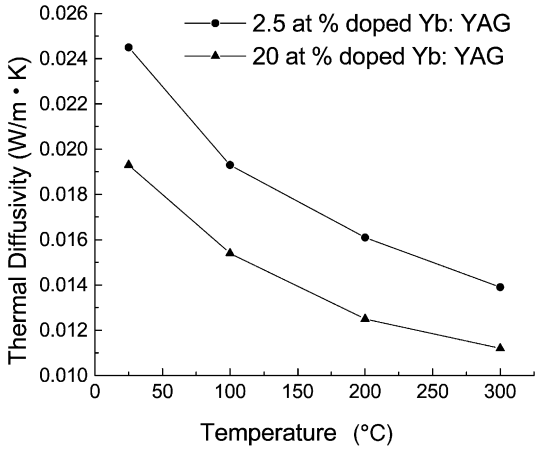

Fig. 2. Thermal diffusivity of 2.5 and 20 at.% doped Yb:YAG.

The change of thermal diffusivity (α) of Yb:YAG with the increase of temperature is shown in Fig. 2, and we can see the apparent influence of the Yb^{3+} doping concentration on thermal diffusivity. At room temperature while the doping concentration of Yb^{3+}, ion increases from 2.5 to 20 at.%, α decreases by as much as 27%, from 0.0245 to 0.0193 cm^2/s. When compared with 1 at.% doped Yb:YAG [8], it decreases by almost 50%. From Fig. 2, we also can see that with the change of temperature thermal diffusivity will decrease, too, and its reduction occurs more slowly at higher temperature.

From α and C_p, thermal conductivity (λ) can be calculated using following equation:

$$\lambda = \alpha \rho C_p \quad (1)$$

Here, ρ is the density of Yb:YAG crystal. The thermal conductivity of different Yb:YAG at different temperature are listed in Table 1. For the convenience of comparison, thermal conductivity of pure YAG [9,10] is listed in Table 1 at the same time. It shows that after doped with Yb^{3+} ion the thermal conductivity value of YAG decreases greatly at room temperature, especially at high doping level. The thermal conductivity of Yb:YAG decreases with the increase in temperature.

The reduction of thermal conductivity at a higher doping concentration is regarded as the result of changes of vibrational modes, which will be discussed in Section 3.3. In Yb:YAG crystals, there is no free electron, so the main mechanism of heat transfer in Yb:YAG is the heat transfer by phonon. Therefore, the changes of lattice vibration directly influence the thermal conductivity of Yb:YAG.

The deterioration of thermal properties of high-doped Yb:YAG will more easily lead to thermooptic aberrations, lensing and birefringence. Therefore, in order to acquire high-beam quality and stable laser output from high-doped Yb:YAG media, efficient cooling system must be adopted.

3.2. The absorption spectra

The measured absorption spectra between 850 and 1100 nm for different Yb^{3+} concentration Yb:YAG crystals are presented in Fig. 3. From Fig. 3, we can see that there are three absorption band of Yb:YAG crystals, the main absorption band centered at 940 nm with an FWHM of about 22 nm. The other two absorption bands centered at 913 and 968 nm, respectively. The concentrations of crystals can also be determined from the absorption spectra of different Yb-doped Yb:YAG crystal. Fig. 4 is the wavelengths of the absorption peak at about 940 nm for Yb:YAG with different concentration. From Figs. 3 and 4, little shifts of absorption peaks at about 940 nm, which usually is pumping wavelength, can be observed, and the absorption peak of highly doped Yb:YAG crystal shifts to shorter wavelength.

The reason leading to the peak shift may be the lattice deformation caused by higher doping concen-

Table 1
Thermal conductivity of Yb:YAG and YAG

		Temperature (K)					
	Sample	200	≈ 300	373	473	573	Ref.
Thermal conductivity	20 at.%		4.74	4.12	3.61	3.45	This work
(W/m K)	2.5 at.%		6.07	5.19	4.60	4.14	This work
	YAG	21	13				[9]
	YAG	16	10.3				[10]

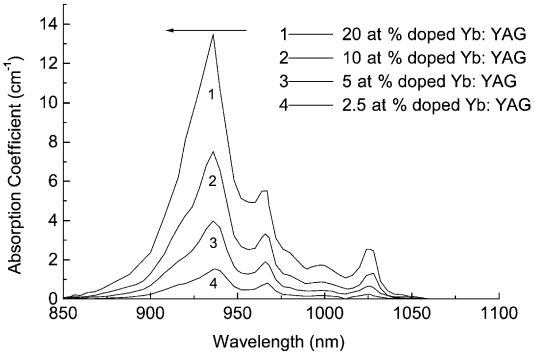

Fig. 3. Absorption band of Yb:YAG with Yb^{3+} concentration from 2.5 to 20 at.%.

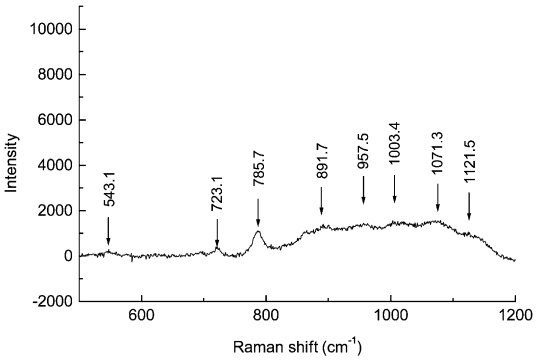

Fig. 5. Raman spectra of lattice vibrational modes in Yb:YAG (5 at.%). The pump source was vertical to the (111) face.

tration of Yb^{3+}. Lattice deformation increases the splitting of electronic manifold, leads to the shift of absorption peak. X-ray diffraction results confirmed our conjecture of lattice deformation. X-ray diffraction results show that the lattice parameter of 30 at.% doped Yb:YAG is 11.978 Å while it is 12.005 Å for pure YAG. The measured lattice parameter of pure YAG is in good agreement with that (12.008 Å for pure YAG crystal) found in JCPDS Card. Because the effective radius of Yb^{3+} is smaller than Y^{3+}, which is replaced by Yb^{3+}, the result is reasonable. This confirms that our measurement is valid.

The shift of the absorption peak at about 940 nm will affect the laser performance. Although the absorption bandwidth [FWHM] centered at 940 nm is about 22 nm, the absorption peak shift should be considered in laser experiment of Yb:YAG crystal. The mismatching of pump wavelength and absorption wavelength will lead to the reduction of laser efficiency.

3.3. The result of Raman spectra

Figs. 5 and 6 show the Raman spectra of Yb:YAG with concentration of 5 at.% and 30 at.%. The pump source was vertical to the (111) face of Yb:YAG crystals. In Fig. 5, when Yb^{3+} concentration is 5 at.%, the Raman shift at 786 cm^{-1} can be observed. In heavily doped Yb:YAG crystals, this lattice vibrational mode disappears. Because there is a line at about 786 cm^{-1} in the spectrum of YAG [11] and low-doped

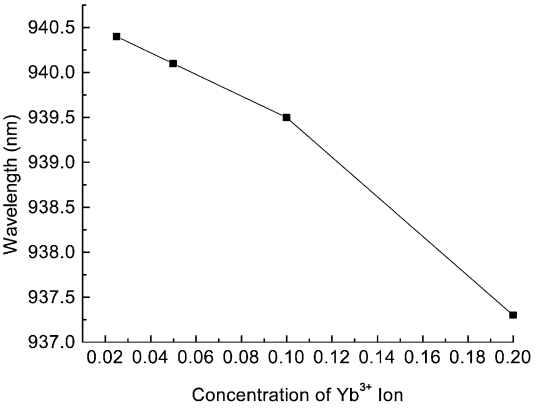

Fig. 4. The relationship between the absorption peak at about 940 nm and the concentration of Yb^{3+} ion in Yb:YAG.

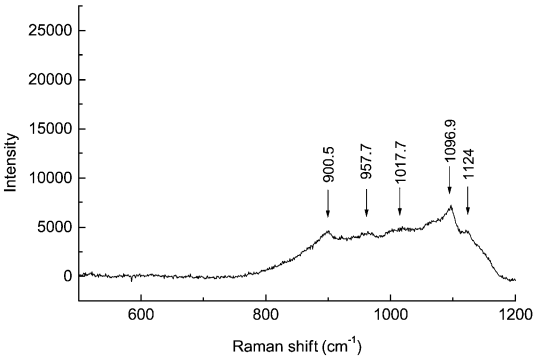

Fig. 6. Raman spectra of lattice vibrational modes in 30 at.% doped Yb:YAG. The pump source was vertical to the (111) face.

Yb:YGG [12] (2–5 at.%), we assign this vibrational mode to the vibration of Y^{3+}–O^{2-}. The disappearance of this line at high Yb^{3+} ion concentration confirms this surmise. In Yb:YAG crystals, the Yb^{3+} take the place of Y^{3+}, which is on the site of dodecahedral sites. Because the effective radius of Yb^{3+} is smaller than that of Y^{3+} (0.985 vs. 1.019 Å), this will lead to lattice deformation in the heavily doped Yb:YAG. It is probably lattice deformation that causes vibrational modes inactive for Raman Scattering.

Figs. 7 and 8 are the Raman spectra of the same samples but pumped in different direction. The laser pump resource was vertical to the face of $(1\bar{1}0)$. From the Raman shift of low-doped crystal (Fig. 6), we can observe a line at 546 cm^{-1}. In the Raman spectra of low doping level Yb:YGG, this line can also be observed [12]. Since there are no such lines in the spectra of Nd:YAG, Eu:YGG, Koningstein [12] regards it as a vibrational mode related to Yb^{3+} ion in YGG. In Yb:YAG, Buchanan et al. [13] think that the strongest vibronic emissions terminate on levels near 547 and 566 cm^{-1}. It should be noted that the line at 546 cm^{-1} also disappears when the doping concentration is high (Fig. 7). So this line should caused by the vibration of Yb–O. Like the line at 786 cm^{-1} for pure YAG or low-doping Yb:YAG crystals, the lattice deformation of the highly doped Yb:YAG leads to the change of crystal symmetry, and results in the change of vibrational modes. Because the ytterbium systems mostly have large vibronic components to their transitions, the disappearance of this line probably influences the spectra.

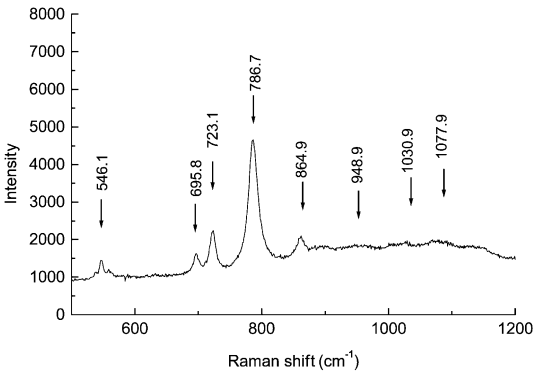

Fig. 7. Raman spectra of lattice vibrational modes in 5 at.% doped Yb:YAG. The pump source was vertical to the $(1\bar{1}0)$ face.

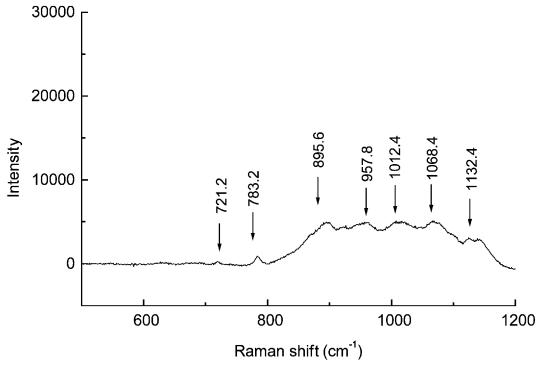

Fig. 8. Raman spectra of lattice vibrational modes in 30 at.% doped Yb:YAG. The pump source was vertical to the $(1\bar{1}0)$ face.

In pure YAG, there are 25 Raman active vibrational modes from theory calculation, and 23 can be observed in the Raman spectra from 0 to 900 cm^{-1} [11]. After doping with Yb^{3+}, five to six lines can be found in the 850–1100 cm^{-1} region and these lines are attributed to the Yb–O vibration. Comparison of the Raman spectra of 5 at.% doped and 30 at.% doped Yb:YAG reveals that the frequency of the lines between 850 and 1100 cm^{-1} increases at higher Yb^{3+} concentrations. For instance, in Fig. 4 the frequency of the line, which is at 891.7 cm^{-1} for low-doped Yb:YAG crystals, becomes 900.5 cm^{-1} at high doping concentration and other lines' frequency increases, too.

Generally, non-radiative relaxation between the Yb^{3+} and the host crystal is regarded as the multiphonon process. Therefore, the changes of lattice vibration will influence the interaction between the Yb^{3+} ion and the host, and at last have some effects on the spectra and laser performance of Yb:YAG crystal. Further research should be done to investigate the influence of vibration changes.

4. The influence on laser output

Our research reveals that some properties of Yb:YAG have been changed at higher ytterbium concentrations. With the goal of exploring the influence of Yb^{3+} concentration on the laser performance, lasers of Yb:YAG with different concentrations were demonstrated. The schematic of the experiment is shown in Fig. 9. The Ti:Sapphire laser with a beam diameter approximately 3 mm is focused into the Yb:YAG with

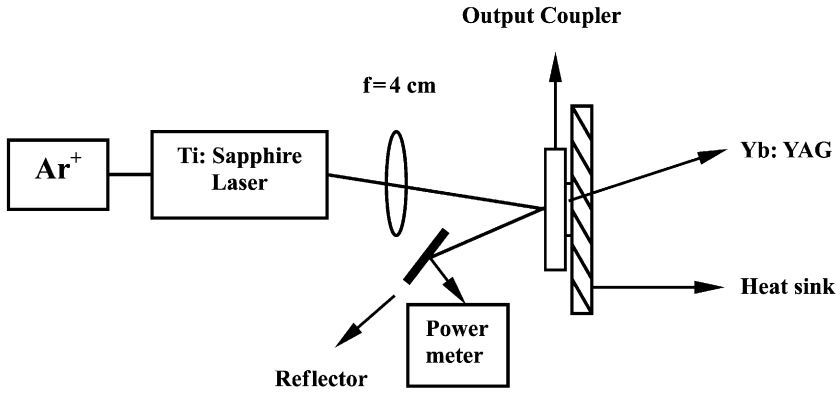

Fig. 9. Experimental set-up of Ti:Sapphire pumped Yb:YAG thin disk laser.

a 40-mm focal length lens. The front side of the cavity lens is of high transmission for pump wavelength at 940 nm and the back side has a high transmission for the wavelength at 940 nm and high reflectivity for laser wavelength at 1053 nm. The Yb:YAG gain element was coated on one face with a mirror with high transmission at 940 and 1053 nm. The other face, which was mounted to a copper heat sink, was coated with high reflectivity coating at 940 mm and high reflectivity coating at 1053 nm. The reflectivity of output coupler is 98.82%.

In Table 2, the data of our laser experiments are listed. For the crystal of the same thickness (1 mm), with the increase of the concentration the slope efficiency increases, from 19% for the 5 at.% doped to 32% for the 10 at.% doped, when the dopant concentration is moderate. But when the Yb^{3+} concentration reaches as high as 20 at.%, the efficiency decreases to 26%. We consider the reduction of laser output efficiency as the result of the property changes of Yb:YAG under high concentration. At low dopant level, there is not enough gain for Yb^{3+} ion and we obtain laser output with relatively low slope efficiency. For the heavily doped Yb:YAG crystals, we regard the low efficiency as the result of the changes of the thermal properties, spectra properties, and others influencing the laser output.

Table 2
The laser properties of Yb:YAG crystal

Yb^{3+} concentration (at.%)	Thickness (mm)	P_{abs} (mW)	P_{out} (mW)	η (%)	Extrapolated threshold (mW)
5	1.0	784	110	19	205
10	1.0	792	206	32	148
20	1.0	784	138	26	253
	0.5	784	225	35	141
30	0.5	629	168	35	149

The Yb^{3+} ion concentration has similar influence on the extrapolated threshold. When the dopant level is low, the threshold is high without enough gain of Yb^{3+} ion, and when the Yb^{3+} concentration is 20 at.%, the threshold is higher than that of 10 at.% doped Yb:YAG caused probably by changes of the properties.

The outputs of 20 at.% doped and 30 at.% doped crystals with the thickness of 0.5 mm also reflect that at high doping rate the Yb^{3+} concentration influence the laser performance of Yb:YAG. Therefore, the Yb^{3+} concentration of Yb:YAG should not be too high in order to obtain stable, high-efficiency laser output.

5. Conclusion

In conclusion, the thermal, absorption spectra and the Raman spectra of Yb:YAG with different concentrations of Yb^{3+} are measured. Our studies show that doping concentration of Yb^{3+} influences the thermal, spectra properties and lattice vibration. At high doping level, the thermal conductivity of Yb:YAG decreases greatly, and the absorption band centered at about 940 nm shifts to shorter wavelength. Comparison of the Raman spectra for low- and high-doped crystals reveals that vibrational modes of Yb:YAG have changed at high doping levels, with some vibrational modes dis-

appearing and some modes' frequency changing. The influence of Yb^{3+} concentration on laser output is also investigated and it shows that for heavily doped Yb:YAG crystal, laser performance has been affected.

References

[1] H.K. Choi, C.A. Wang, Appl. Phys. Lett. 57 (1990) 321.
[2] D.P. Bour, G.A. Evans, D.P. Gilbert, J. Appl. Phys. 65 (1989) 3340.
[3] L.D. DeLoach, S.A. Payne, L.L. Chase, et al., IEEE J. Quantum Electron. 29 (4) (1993) 1179.
[4] D.C. Brown, IEEE J. Quantum Electron. 33 (5) (1997) 861.
[5] T.Y. Fan, IEEE J. Quantum Electron. 28 (12) (1992) 2692.
[6] T.Y. Fan, IEEE J. Quantum Electron. 29 (6) (1993) 1457.
[7] A.R. Reinber, L.A. Reseberg, R.M. Brown, R.W. Wacker, W.C. Holton, Appl. Phys. Lett. 19 (1) (1971) 11.
[8] H. Bruesselbach, D.S. Sumida, Opt. Lett. 21 (7) (1996) 480.
[9] P.H. Klein, W.J. Croft, J. Appl. Phys. 38 (4) (1967) 1603.
[10] G.A. Slack, D.W. Oliver, Phys. Rev. 4 (2) (1971) 592.
[11] J.P. Hurrell, S.P.S. Porto, I.F. Chang, S.S. Mitra, R.P. Bauman, Phys. Rev. 173 (3) (1968) 851.
[12] J.A. Konlingstein, J. Chem. Phys. 46 (7) (1967) 2811.
[13] R.A. Buchanan, K.A. Wickersheim, J.J. Pearson, G.F. Herrmann, Phys. Rev. 159 (2) (1967) 245.